Correlations in Abelian lattice gauge field models: A microscopic coupled-cluster treatment

R. F. Bishop, A. S. Kendall, L. Y. Wong, and Y. Xian
Department of Mathematics, University of Manchester Institute of Science and Technology (UMIST), P.O. Box 88, Manchester M60 1QD, England
(Received 26 October 1992)

An *ab initio* formulation of microscopic quantum many-body theory, namely, the coupled-cluster method (CCM), is applied to the lattice gauge models, $Z(2)$ in $2+1$ dimensions, and U(1) in $1+1$ and $2+1$ dimensions. Both mode-mode couplings and plaquette-plaquette correlations are considered. In particular, within the one-plaquette approximation for the U(1) model, the CCM is able to include mode couplings of arbitrarily high order. It therefore reproduces essentially the *exact* numerical results for the equivalent Mathieu problem. These include the ground-state, plaquette, and excitation energies as functions of the coupling constant. Two-plaquette equations are solved by local approximations for both the U(1) and $Z(2)$ models, and the results are impressive. Detailed comparisons with other methods, particularly perturbation theory, are made and discussed, with emphasis on the nonperturbative nature of the problem.

PACS number(s): 11.15.Ha, 03.65.Ca, 03.70.+k, 11.15.Tk

I. INTRODUCTION

From several points of view the application of *ab initio* techniques from microscopic quantum many-body theory (QMBT) to problems in gauge field theory appears to be particularly timely. Thus, firstly, enormous progress has been made in QMBT over the last ten years or so. The field has both deepened at the level of formal developments and broadened in its range of successful applications to problems of physical and chemical interest. Two methods have especially come to the forefront because of their demonstrated versatility, their ability to achieve very high accuracy at attainable levels of approximations, and their capacity for systematic improvement. These are the method of correlated basis functions (CBF's) [1], and the coupled-cluster method (CCM) [2–12]. They are widely recognized as providing the two most powerful microscopic formulations currently available for dealing at an *ab initio* level with fundamental problems of QMBT.

Secondly, strong pessimism and reservations have been voiced by Wilson [13] concerning the development still needed within lattice quantum chromodynamics (QCD) before there can occur meaningful comparisons with experiment. For example, he quantifies the existing gap between theory and experiment by suggesting that an increase in computational power of at least a factor of 10^8 *and* equally powerful algorithmic or methodological advances are both needed. Wilson further recommends the lattice gauge community to look especially to the field of quantum chemistry for new ideas and additional inspiration, particularly since both fields share a common concern with many-fermion systems interacting via long-range (unscreened) forces.

Our own starting point is that what is valid for quantum chemistry in particular is equally valid for QMBT in general. We also note within this context that one of the methods currently applied very widely within quantum chemistry is the CCM. For example, the very high accuracy required nowadays for the calculation of parity violation in atoms or for the calculation of molecular energy differences of chemical significance, requires extremely accurate treatments of the electronic correlations [14]. The CCM is ideally suited for such applications. Indeed, it is now widely recognized as the method of first choice in terms of power and accuracy for calculations of, for example, ionization potentials, electron affinities, Auger spectroscopy, excitation energies, and energy gradients (for use, for example, in searching potential energy surfaces to predict vibrational spectra, or to locate transition states in decomposition reactions). By now, many atoms and molecules have been studied, with state-of-the-art calculations being performed on molecules with up to about 80 active electrons [14].

Apart from its manifest achievements in quantum chemistry, the CCM has successfully been applied to a plethora of other physical problems. Other many-fermion applications, for example, have included problems in nuclear physics, both for finite nuclei [6,8] and infinite nuclear matter [15], and the electron gas [5,16]. The latter provides a typical example of the accuracy of the method. By comparison with the essentially exact Green's-function Monte Carlo results available for this case, the CCM is seen to give correlation energies per electron accurate to less than one millihartree (or $<1\%$) over the entire range of densities appropriate to real metals. No other technique of QMBT has bettered or equaled this accuracy, for what is still one of the most well studied of all many-body problems. Other applications of the CCM include various models such as the Lipkin-Meshkov-Glick quasispin model [17], and anharmonic spin models [18]. Applications of closer relevance to particle physics include anharmonic oscillators and other single-mode $(0+1)$-dimensional field theories [19,20], Φ^4 field theory [21], and a model field theory of pions and nucleons interacting via an isospin-invariant

pseudoscalar coupling [22]. All of these and other applications of the CCM have been reviewed recently in Ref. [12].

Finally, we note that the range of applications of the CCM has recently been extended to include various models of strongly interacting spins or fermions on a regular lattice, of interest in condensed matter physics. Successful applications have been made over the last few years to, for example, the body-centered cubic (bcc) phase of solid ^{3}He [23], the half-filled Hubbard model on a square lattice [24], and various spin models which exhibit antiferromagnetism on a bipartite lattice in one, two, and three dimensions, including the anisotropic Heisenberg (or XXZ) Hamiltonian [23,25]. In particular, for the latter model, it has been shown [25], for example, how in a specified localized approximation scheme the results of perturbation theory (in the anisotropicity parameter) about the Ising limit can readily be reproduced in such a way that the resulting CCM hierarchy represents a natural extension of its perturbation theory counterpart, in the sense of a well-defined analytic continuation or resummation. Numerical results indicate rapid convergence, even in the regime where perturbation theory diverges badly (beyond the observed phase transition). Furthermore, it has also been shown [25] how the CCM can, in an alternative approximation scheme which retains correlations between the spins of arbitrarily long range, give a qualitatively correct description of the entire Heisenberg-Ising phase, including (a prediction of) the critical point where a phase transition occurs.

For all of the above reasons, it seems worthwhile to attempt to apply similar CCM techniques to lattice gauge field theories. The present paper presents our preliminary results in this respect for the Abelian models $Z(2)$ in $2+1$ dimensions and U(1) in $1+1$ and $2+1$ dimensions. Henceforth, we refer to these as 1D and 2D cases, respectively. The general CCM formalism as applied to both models is first outlined in Sec. II. Results for the ground-state energy for the U(1) model are then discussed in Secs. III and IV, respectively, within the so-called one- and two-plaquette approximations in a systematic hierarchy of truncations described in Sec. II. Results for the so-called plaquette energy for the U(1) model are discussed in Sec. V. Similar ground-state results for the $Z(2)$ model are given in Sec. VI, and finally in Sec. VII the CCM description of the excited states of both models is discussed. In all cases, detailed comparisons are made with the results from perturbation theory and other methods. We conclude with a summary and discussion in Sec. VIII.

II. COUPLED-CLUSTER FORMALISM FOR U(1) AND $Z(2)$ MODELS

In order to describe the correlations in a many-body system the coupled-cluster method (CCM) starts from a suitable reference state. This is usually (but not always) the properly symmetrized, noninteracting many-body state composed of some single-particle wave functions chosen to be the eigenstates of an appropriate one-body Hamiltonian. The correlations present in the physical system are then incorporated via many-body excitations from this reference state. In this respect the CCM is similar to perturbation theory. Nevertheless, the CCM is highly nonperturbative, since the correlation operator actually takes the form of an exponentiated function [2,12], as is by now rather well known, and as we shall see in detail below.

Since the CCM has been well reviewed many times in the past, we refer the reader to the literature for both a general description of the method (and see, for example, Ref. [12] and the references cited therein) and its previous applications to spin-lattice problems in particular [25]. In this section we concentrate on the specific applications to the U(1) and $Z(2)$ lattice gauge models.

A. The U(1) model

The Hamiltonian for the U(1) lattice gauge-field theory is usually written as

$$H=-\frac{1}{2}\sum_l \frac{\partial^2}{\partial A_l^2}+\lambda\sum_p (1-\cos B_p)\ , \tag{2.1}$$

where the first summation is over all links l of the lattice, and the second over all plaquettes p, λ is the coupling constant, $0\le\lambda<\infty$, A_l is a vector potential defined on the link l, whereas the magnetic field B_p is a plaquette variable defined by the four values of A_l with $l\in p$, i.e., $B_p\equiv A_1+A_2-A_3-A_4$, where the order and the sign of A_l ($l\in p$) are conventionally chosen as shown in Fig. 1. We can easily express H in terms of the plaquette variables alone for any dimensionality. Since we consider only the cases of $1+1$ dimensions (1D chain, i.e., a linear array of plaquettes) and $2+1$ dimensions (2D square lattice) in this paper, we quote the corresponding Hamiltonians,

$$H=\sum_p \left[-2\frac{\partial^2}{\partial B_p^2}+\lambda(1-\cos B_p)\right]+\frac{1}{2}\sum_{p,\rho}\frac{\partial^2}{\partial B_p \partial B_{p+\rho}}\ , \tag{2.2}$$

where ρ is a lattice vector connecting nearest-neighboring plaquettes of the lattice. In 1D ρ has two values, while in 2D it has four. (Equation (2.2) is identical to Eq. (2) of Ref. [26] in the 2D square lattice case.) The Hamiltonian of Eq. (2.2) is invariant under the transformation $B_p\to B_p+2n\pi$, with n integral. Hence the space of B_p is compact ($-\pi\le B_p\le\pi$, for all p).

The Schrödinger equation for Eq. (2.2) reduces in the case of a single plaquette to the Mathieu equation:

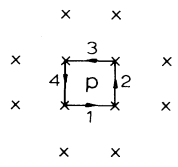

FIG. 1. A single plaquette. The order of the four links of the plaquette is indicated, as used in the definition of plaquette variables.

$$-2\frac{d^2}{dB^2}\psi_n(B)+\lambda(1-\cos B)\psi_n(B)=e_n\psi_n(B)\ ,$$

$$-\pi\le B\le\pi\ . \quad (2.3)$$

In view of the fact that small-λ perturbation theory for the ground state of the Mathieu equation is well known to have a finite radius of convergence, it is pertinent to consider the simpler problem of its so-called strong-coupling ($\lambda\to 0$) limit first. This simple unperturbed Hamiltonian $H_0=-2d^2/dB^2$ with $-\pi\le B\le\pi$ has two sets of eigenstates: namely, $\{\cos mB;\ m=0,1,2,\ldots\}$ with even parity, and $\{\sin mB;\ m=1,2,\ldots\}$ with odd parity. The ground state of H_0 is clearly just a constant. We now use these simple strong-coupling single-plaquette wave functions to construct both the ket and bra states in terms of a CCM analysis.

The noninteracting reference state $|\Phi\rangle$ is hence simply a constant. The exact many-body ket ground state (GS) of the U(1) Hamiltonian of Eq. (2.2) is then taken in the CCM form

$$|\Psi_0(\{B_p\})\rangle=e^{S(\{B_p\})}|\Phi\rangle\ ,$$

$$S(\{B_p\})=\sum_{k=1}^{N_p}S_k(\{B_p\})\ , \quad (2.4)$$

where N_p is the total number of plaquettes in the lattice and where the k-body correlation operators S_k are decomposed as

$$S_1=\sum_{n=1}^{\infty}\sum_{p=1}^{N_p}\mathcal{S}_p(n)\cos(nB_p)\ , \quad (2.5a)$$

$$S_2=\frac{1}{2!}\sum_{n_1,n_2=1}^{\infty}{\sum_{p_1,p_2=1}^{N_p}}'[\mathcal{S}^{(1)}_{p_1p_2}(n_1,n_2)\cos(n_1B_{p_1})\cos(n_2B_{p_2})+\mathcal{S}^{(2)}_{p_1p_2}(n_1,n_2)\sin(n_1B_{p_1})\sin(n_2B_{p_2})]\ , \quad (2.5b)$$

and similarly for the higher-order partitions S_k with $k>2$. The coefficients $\{\mathcal{S}_{p_1\ldots}(n_1,\ldots)\}$ are to be determined by the CCM coupled equations discussed below, and the prime on the summation in Eq. (2.5b) excludes the terms with $p_1=p_2$.

For reasons which have been described many times in the past [12] the bra GS, $\langle\tilde{\Psi}_0|$, in the CCM parametrization is not taken as the manifest Hermitian conjugate of $|\Psi_0\rangle$. Instead, it is parametrized in the form

$$\langle\tilde{\Psi}_0(\{B_p\})|=\langle\Phi|\tilde{S}(\{B_p\})e^{-S(\{B_p\})}\ ,$$

$$\tilde{S}=1+\sum_{k=1}^{N_p}\tilde{S}_k(\{B_p\})\ , \quad (2.6)$$

where $S=S(\{B_p\})$ is as given above in Eqs. (2.4) and (2.5), and $\tilde{S}_k$ is similarly defined as in Eqs. (2.5) except that all coefficients $\{\mathcal{S}_{p_1\ldots}(n,\ldots)\}$ are replaced by the corresponding $\{\tilde{\mathcal{S}}_{p_1\ldots}(n_1,\ldots)\}$. We note that both $|\Psi_0\rangle$ and $\langle\tilde{\Psi}_0|$ are explicitly invariant under the transformation $B_p\to B_p+2\pi$. As befits the GS, they have also been constructed to have even parity under interchange of the sign of all the variables $\{B_p\}$.

We define an inner product of wave functions $\langle\tilde{g}(\{B_p\})|$ and $|f(\{B_p\})\rangle$ as

$$\langle\tilde{g}|f\rangle=\int_{-\pi}^{\pi}\prod_{p=1}^{N_p}\left[\frac{dB_p}{2\pi}\right]\tilde{g}f\ , \quad (2.7a)$$

and the expectation value of an operator $\theta=\theta(\{B_p\},\{d/dB_p\})$ with respect to the conjugate states $|f\rangle$ and $\langle\tilde{f}|$ as

$$\bar{\theta}\equiv\langle\tilde{f}|\theta|f\rangle=\int_{-\pi}^{\pi}\prod_{p=1}^{N_p}\left[\frac{dB_p}{2\pi}\right]\tilde{f}\theta f\ . \quad (2.7b)$$

The normalization condition $\langle\Phi|\Phi\rangle=1$ then gives Φ equal to unity. The CCM equations for the correlation coefficients of Eq. (2.5) are now derived from the condition that the GS expectation value of the Hamiltonian of Eq. (2.2),

$$\bar{H}=\langle\tilde{\Psi}_0|H|\Psi_0\rangle=\langle\Phi|\tilde{S}e^{-S}He^{S}|\Phi\rangle\ , \quad (2.8)$$

should be stationary with respect to variations in *both* complete sets of bra- and ket-state coefficients. Thus, for example, the one-plaquette coefficients $\{\mathcal{S}_p(n),\tilde{\mathcal{S}}_p(n)\}$ are determined by the variational principle, respectively:

$$\frac{\delta\bar{H}}{\delta\tilde{\mathcal{S}}_p(n)}=0=\frac{\delta\bar{H}}{\delta\mathcal{S}_p(n)}\ . \quad (2.9)$$

The equations for the two- and higher-order many-body coefficients are similarly given by the corresponding stationary conditions for $\bar{H}$.

Within the context of the above CCM parameterization there are clearly two distinct kinds of correlations in play. In the first place one has the mode-coupling terms between different modes $\{\cos(nB_p),\sin(nB_p)\}$ specified by the index n. Second, one has the more physical correlations between different plaquettes specified by the indices $\{p_i\}$. Clearly mode coupling is included even at the one-plaquette level (i.e., as specified by S_1 and $\tilde{S}_1$ alone), whereas one needs to include at least S_2 and $\tilde{S}_2$ as well in order to describe plaquette correlations.

We also note that the CCM correlation operators of Eqs. (2.4)–(2.6) do not involve the usual creation and destruction operators as in the more conventional CCM [2,12,25]. This distinct difference is related essentially to the fact that in the lattice gauge systems under consideration there are neither any real particles nor quasiparticles defined. Whereas in more conventional many-body problems one is usually concerned with particle conservation, the primary concern in lattice gauge models is the gauge invariance.

B. The $Z(2)$ model

The Hamiltonian of the $Z(2)$ lattice gauge theory can be written in terms of spin-$\frac{1}{2}$ Pauli matrices σ_α ($\alpha=1,2,3$) as

$$H=-\sum_l \sigma_1(l)-\lambda\sum_p U_p$$

$$\text{with } U_p\equiv\sigma_3(1)\sigma_3(2)\sigma_3(3)\sigma_3(4)\ , \quad (2.10)$$

where as in Eq. (2.1), summations over l and p are over all links and all plaquettes of the lattice, respectively, and where the plaquette variable U_p is defined in the conventional order as shown in Fig. 1.

The so-called strong-coupling ($\lambda\to 0$) limit of Eq. (2.10) is $H_0=-\sum_l\sigma_1(l)$. Hence the model state $|\Phi\rangle$ of the CCM is now taken for this $Z(2)$ gauge theory as the GS of H_0, namely, the state with all spins aligned with respect to the 1 axis, such that

$$\sigma_1(l)|\Phi\rangle=|\Phi\rangle, \quad \forall l\ . \quad (2.11)$$

Exactly as for the U(1) model, the ket and bra GS wave functions $|\Psi_0\rangle$ and $\langle\tilde{\Psi}_0|$ of Eq. (2.10) are formed in terms of the similar correlation operators S and $\tilde{S}$. Hence we may write for the ket GS, by analogy with Eqs. (2.4) and (2.5),

$$|\Psi_0\rangle=e^S|\Phi\rangle, \quad S=\sum_{k=1}^{N_p} S_k\ , \quad (2.12)$$

where the k-body partitions of the correlation operator are now specified as

$$S_k=\frac{1}{k!}\sum_{p_1,p_2,\ldots,p_k=1}^{N_p}{}' \mathcal{S}_{p_1p_2\cdots p_k}U_{p_1}U_{p_2}\cdots U_{p_k}\ , \quad (2.13)$$

where again the prime on the summations indicates that no two indices are the same. The bra GS is similarly specified, by analogy with Eq. (2.6), in the form

$$\langle\tilde{\Psi}_0|=\langle\Phi|\tilde{S}e^{-S}, \quad \tilde{S}=1+\sum_{k=1}^{N_p}\tilde{S}_k\ , \quad (2.14)$$

and where $\tilde{S}_k$ is parametrized exactly as in Eq. (2.13), except with the replacement $\{\mathcal{S}_{p_1\cdots p_k}\}\to\{\tilde{\mathcal{S}}_{p_1\cdots p_k}\}$. Clearly, both $|\Psi_0\rangle$ and $\langle\tilde{\Psi}_0|$ are gauge invariant, as required.

III. U(1) GROUND-STATE ENERGY: ONE-PLAQUETTE SCHEME

In principle, the exact ket and bra ground states of the U(1) and $Z(2)$ lattice gauge model are given by Eqs. (2.4)–(2.6) and (2.12)–(2.14), respectively, where *all* correlation operators $\{S_k,\tilde{S}_k;\ k=1,2,\ldots,N_p\}$ should be included. In practice, one clearly needs to approximate. Different approximation schemes have been developed and tested during the course of the many and diverse applications of the CCM. For example, the most common CCM truncation scheme is the so-called SUBn scheme, in which only those correlations described by the cluster partitions $\{S_k,\tilde{S}_k\}$ with $k\le n$ are included, and those with $k>n$ are set to zero. Another more recent scheme, the so-called LSUBn scheme which takes into account only localized correlations, is also especially suited for lattice systems with local interactions. However, in this section we consider the lowest-order SUB1 approximation only, for which we therefore make the replacements $S\to S_{\text{SUB1}}=S_1$, $\tilde{S}\to\tilde{S}_{\text{SUB1}}=\tilde{S}_1$; and we consider the SUB2 approximation in the next section and the LSUBn scheme for the $Z(2)$ model in Sec. VI.

The retained coefficients $\{\mathcal{S}_p(n),\tilde{\mathcal{S}}_p(n)\}$ are then found as described in Sec. II A, and as given by Eq. (2.9). In particular, the SUB1 GS ket coefficients are clearly obtained by solving the *coupled* set of equations

$$\langle\cos(mB_p)|e^{-S_{\text{SUB1}}}He^{S_{\text{SUB1}}}|\Phi\rangle=0\ , \quad m=1,2,\ldots, \quad (3.1)$$

where the notation involved is as defined by Eqs. (2.7). Although the evaluation of the GS expectation value of an arbitrary operator in this SUB1 approximation would also require the bra GS coefficients $\{\tilde{\mathcal{S}}_p(n)\}$, the GS energy E_g is clearly given in terms of the ket GS coefficients alone as

$$E_g=\langle\Phi|e^{-S_{\text{SUB1}}}He^{S_{\text{SUB1}}}|\Phi\rangle\ . \quad (3.2)$$

In terms of the parametrization of Eq. (2.5a), it is not difficult to derive the explicit SUB1-approximation equations for both the 1D and 2D cases:

$$\sum_{p=1}^{N_p}\left[-\frac{1}{2}\lambda\delta_{m,1}+m^2\mathcal{S}_p(m)+\frac{1}{2}\sum_{n,n'=1}^{\infty}nn'\mathcal{S}_p(n)\mathcal{S}_p(n')(\delta_{m,n+n'}-\delta_{m,|n-n'|})\right]=0, \quad m=1,2,\ldots \quad (3.3)$$

and

$$E_g=\lambda N_p-\sum_{p=1}^{N_p}\sum_{n=1}^{\infty}n^2\mathcal{S}_p^2(n)\ . \quad (3.4)$$

In the thermodynamic limit ($N_p\to\infty$) considered here, the coefficients $\mathcal{S}_p(n)$ are independent of plaquette index p by lattice translational invariance. After extension of the definition of these coefficients to include the negative modes, i.e.,

$$a_m\equiv m\mathcal{S}_p(m), \quad \text{with } a_{-m}=-a_m \text{ and } a_0=0\ , \quad (3.5)$$

we may readily rewrite Eqs. (3.3) and (3.4) as

$$\left[\frac{E_g}{N_p}-\lambda\right]\delta_{m,0}+\frac{1}{2}\lambda(\delta_{m,1}+\delta_{m,-1})-ma_m-\frac{1}{2}\sum_{n=-\infty}^{\infty}a_na_{m-n}=0\ , \quad (3.6)$$

which is valid for all integers m. We may now define an odd function $A = A(B)$ by the Fourier sum

$$A(B) \equiv \sum_{m=-\infty}^{\infty} a_m \sin(mB) , \tag{3.7}$$

whose inverse is given by

$$a_m = \frac{1}{2\pi} \int_{-\pi}^{\pi} dB \; A(B) \sin(mB) . \tag{3.8}$$

It is easy to show that Eq. (3.6) is equivalent to the first-order Riccati equation:

$$\frac{dA}{dB} - \frac{1}{2} A^2 = \frac{E_g}{N_p} - \lambda(1 - \cos B) . \tag{3.9}$$

Finally, the standard substitution

$$A \equiv -\frac{2}{\psi} \frac{d\psi}{dB} \tag{3.10}$$

reduces Eq. (3.9) to the Mathieu equation

$$\left[-2\frac{d^2}{dB^2} + \lambda(1 - \cos B) \right] \psi(B) = \frac{E_g}{N_p} \psi(B) , \tag{3.11}$$

which may be compared with the single-plaquette equation (2.3).

The fact that we regain the Mathieu equation in our SUB1 scheme is not surprising since no multiplaquette correlation effects have been included, and as we and others [27,28] have shown, the single-plaquette problem is equivalent to the Mathieu equation. In fact, this is true for the U(1) models in *any* dimension. Nevertheless, the many-body nature of our system has not been entirely lost, since the eigenvalue in Eq. (3.11) is the intensive quantity, E_g/N_p. Furthermore, one can without too much difficulty go beyond this SUB1 level to include two-plaquette (and higher-order) correlations in our CCM formalism, as considered in the SUB2 scheme in the following section.

For the present purpose, however, we remain at the SUB1 level. In order to solve the coupled equations (3.6), it is natural to define the so-called SUB1(n) subhierarchy in which one retains at the nth level of approximation only those coefficients a_m with $|m| \leq n$, and sets the remainder with $|m| > n$ to zero. Thus, in the SUB1(1) scheme, only the single independent coefficient $a_1 (= -a_{-1})$ is retained. The solution is trivially given as

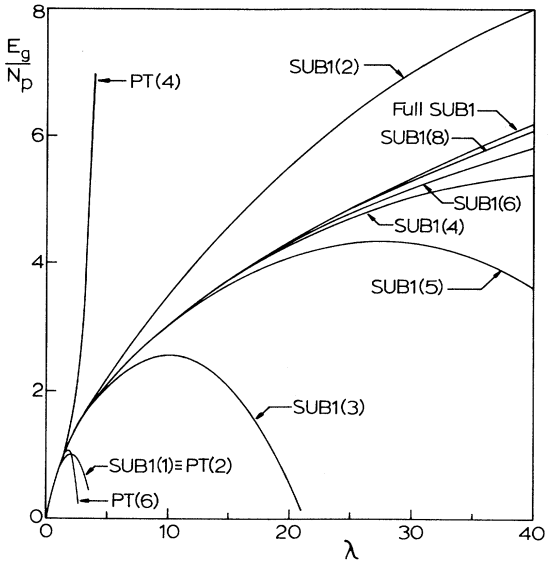

FIG. 2. Ground-state energy per plaquette of the U(1) model as a function of λ for several SUB1(n) approximations, including the full SUB1 scheme which corresponds to the exact solution of the Mathieu problem, and some results from perturbation theory, PT($2n$).

$$a_1 = \frac{1}{2}\lambda, \quad \frac{E_g}{N_p} = \lambda - \frac{1}{4}\lambda^2, \quad \text{SUB1(1)} . \tag{3.12}$$

Similarly in the SUB1(2) approximation one retains only the two independent coefficients a_1 and a_2. The solution to Eq. (3.6) in this case is given by

$$\begin{aligned} a_1 &= (\sqrt{\lambda^2 + \tfrac{64}{27}} + \lambda)^{1/3} - (\sqrt{\lambda^2 + \tfrac{64}{27}} - \lambda)^{1/3} , \\ a_2 &= -\frac{1}{4} a_1^2, \quad \frac{E_g}{N_p} = \lambda - a_1^2 - a_2^2, \quad \text{SUB1(2)} . \end{aligned} \tag{3.13}$$

Solutions for arbitrary n and λ to the general SUB1(n) approximation to Eq. (3.6) are easily obtained numerically by a simple iteration method on a microcomputer. An accuracy of six significant figures, for example, is usually obtained in less than about five iterations. The GS energy per plaquette, E_g/N_p, is shown in Fig. 2 and Table I as a function of λ for several SUB1(n) schemes. The full SUB1 values, which are the *exact* solution of the Mathieu

TABLE I. Ground-state energy per plaquette at various values of λ for the U(1) lattice gauge model within the SUB1(n) schemes with $n = 1, 2, 3, 4, 8, 20$. Under the SUB1(n) approximation the U(1) model is equivalent to the Mathieu problem; and the SUB1(20) results are exact to the accuracy shown for the Mathieu problem.

λ	0.5	1	2	3	5	20
SUB1(1)	0.437 5	0.75	1	0.75	−1.25	−80
SUB1(2)	0.439 123	0.772 689	1.249 117	1.608 770	2.209 359	5.525 510
SUB1(3)	0.439 117	0.772 425	1.242 552	1.578 798	2.061 439	0.553 501
SUB1(4)	0.439 117	0.772 431	1.243 018	1.582 758	2.099 494	4.273 716
SUB1(8)	0.439 117	0.772 431	1.243 021	1.582 804	2.099 974	4.335 206
SUB1(20)	0.439 117	0.772 431	1.243 021	1.582 804	2.099 977	4.343 306

equation (2.3), are actually well represented, to the level of accuracy shown, by the SUB1(20) results for the whole range of λ displayed. The convergence with index n of the SUB1(n) results to the full SUB1 limit is clearly quite rapid, even in the large-λ (weak-coupling) limit.

It is also interesting to compare our SUB1(n) scheme results with the counterparts for the Mathieu problem from perturbation theory in the strong-coupling limit. Up to 14th order in this limit, the GS eigenvalue of Eq. (2.3) is given by [29]

$$\epsilon_0 \underset{\lambda\to 0}{\sim} \lambda-\frac{1}{4}\lambda^2+\frac{7}{256}\lambda^4-\frac{29}{4608}\lambda^6+\frac{68\,687}{37\,748\,736}\lambda^8 -\frac{123\,707}{209\,715\,200}\lambda^{10}+\frac{8022\,167\,579}{39\,137\,889\,484\,800}\lambda^{12} -\frac{286\,241\,141\,477}{3835\,513\,169\,510\,400}\lambda^{14}+O(\lambda^{16}) . \tag{3.14}$$

We have explicitly verified [30] that in this limit the SUB1(7) approximation for E_g/N_p exactly reproduces this series to the order shown. In general, the $\lambda\to 0$ limiting form of the GS energy in SUB1(n) approximation exactly reproduces the result from $2n$th-order perturbation theory [PT($2n$)]. Indeed, the SUB1(n) scheme actually provides a very efficient way to generate the coefficients of the terms in the perturbation treatment of the Mathieu problem. A more detailed comparison of the SUB1(n) and PT($2n$) results for the GS energy is provided by Fig. 2, where we see clearly that the perturbation results are very poor for $\lambda > 1.5$. In fact, as given in Ref. [29], the radius of convergence for the series of Eq. (3.14) is no greater than $\lambda_0 = 1.468\,77$, accurate to five decimal places.

Clearly, the range of validity of the SUB1(n) results extends to values well above $\lambda=\lambda_0$. The accuracy of different orders of perturbation theory as a function of λ is shown more explicitly in Fig. 3. The accuracy $\mathcal{A}$ of a quantity E is, roughly speaking, the number of significant figures of the approximate result E_a compared with its exact counterpart E_e. It is defined more precisely as

$$\mathcal{A} \equiv \log_{10}\left|\frac{E_e}{E_e-E_a}\right| . \tag{3.15}$$

Figure 3 exhibits rather well the fact that the series of Eq. (3.14) has a finite radius ($\leq \lambda_0$) of convergence.

By contrast, the accuracy of the comparable SUB1(n) results is displayed in the same way in Fig. 4. It is clear that these results represent a very natural extension of the PT($2n$) approximations. They comprise, in effect, a well-defined analytic continuation or resummation of the PT($2n$) results, within the context of a systematic hierarchy of approximations. In this sense, the SUB1(n) scheme may be contrasted with alternative rather *ad hoc* approaches for extending the range of validity or the accuracy of similar PT(n) sequences. These include Padé approximant and related techniques.

In fact, the nonperturbative nature of the Mathieu equation has long made it a testing ground for different techniques to attack lattice gauge theories. These have included variational methods [31], and use of the Lanczos algorithm to improve upon them [32]. More generally, the Hamiltonian version of the U(1) lattice gauge model considered here has also been investigated by such other methods as strong-coupling perturbation theory [33], finite lattice calculations [34], various Monte Carlo techniques [27,35,36], variational approaches [37], the method of correlated basis functions [26], and a block renormalization-group approach [38]. Most of these alternative techniques have demonstrated the necessity to include higher-order mode couplings. Our own results for the SUB1(n) scheme have clearly proven the efficacy of

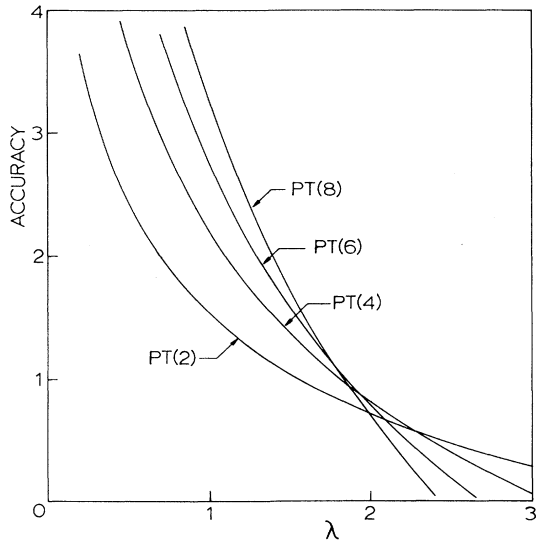

FIG. 3. The accuracy, defined in Eq. (3.15), as a function of λ for the ground-state energy, e_0, of the Mathieu equation (2.3) calculated in the nth-order strong-coupling ($\lambda\to 0$) perturbation theory, PT(n) ($n=2,4,6,8$), compared to the exact result. The radius of convergence of PT is $\leq \lambda_0 = 1.468\,77$ [29].

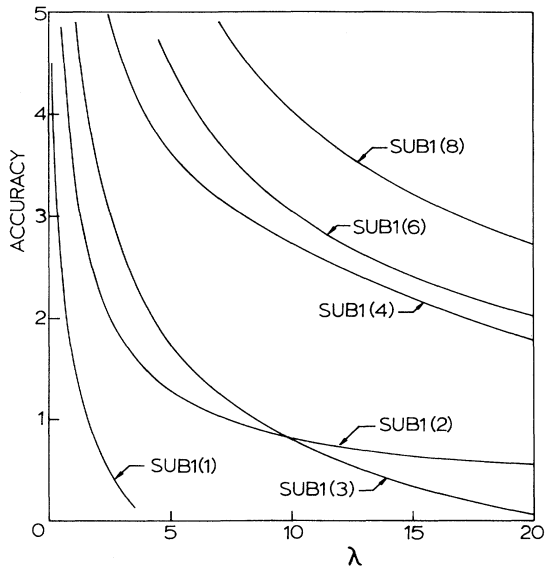

FIG. 4. Same as Fig. 3 but with the results from our SUB1(n) schemes.

the CCM for handling the nonperturbative sector of the U(1) lattice gauge model.

As stated before, it is straightforward to include another kind of correlation effect in the CCM, namely, the physical plaquette correlations. This is the subject of the next section.

IV. U(1) GROUND-STATE ENERGY: TWO-PLAQUETTE SCHEME

In the previous section one-plaquette equations (3.1) are derived rather easily and solved by a simple numerical technique. The two-plaquette equations can also be derived in a similar manner but with more effort. We thus extend our discussion to the SUB2 scheme, in which the correlation operator S in Eq. (2.4) is truncated as

$$S \rightarrow S_{\mathrm{SUB2}} = S_1 + S_2 \ , \tag{4.1}$$

where S_1 and S_2 are written as in Eq. (2.5). Similar to Eqs. (2.9) and (3.1) of the one-plaquette equation in the SUB1 scheme, in replacing S_{SUB1} with S_{SUB2}, one can derive the two-plaquette equations, in addition to the one-plaquette equation. They are given respectively, by,

$$\langle \cos(m_1 B_{p_1}) \cos(m_2 B_{p_2}) | e^{-S_{\mathrm{SUB2}}} H e^{S_{\mathrm{SUB2}}} | \Phi \rangle = 0 \ ,$$
$$m_1, m_2 = 1,2,\ldots, \quad p_1 \neq p_2 \ , \tag{4.2}$$

for the coefficients $\mathcal{S}^{(1)}_{p_1 p_2}(n_1, n_2)$, and

$$\langle \sin(m_1 B_{p_1}) \sin(m_2 B_{p_2}) | e^{-S_{\mathrm{SUB2}}} H e^{S_{\mathrm{SUB2}}} | \Phi \rangle = 0 \ ,$$
$$m_1, m_2 = 1,2,\ldots, \quad p_1 \neq p_2 \ , \tag{4.3}$$

for the coefficients $\mathcal{S}^{(2)}_{p_1 p_2}(n_1, n_2)$. The one-plaquette equations in this SUB2 approximation, analogous to Eq. (3.1) in the SUB1 approximation, are simply those obtained from Eq. (4.2) by setting $m_2 = 0$, with $m_1 = 1,2,\ldots$. Again, the equations are highly coupled.

We have derived the full equations in this SUB2 scheme. Obviously, they are quite involved. In the following we consider some partial approximations within this SUB2 scheme. First we need to simplify the notations for the two-plaquette coefficients. Using the translational invariance, we can write

$$\mathcal{S}^{(1)}_{p_1 p_2}(n_1, n_2) \equiv b_r(n_1, n_2) \ ,$$
$$\mathcal{S}^{(2)}_{p_1 p_2}(n_1, n_2) \equiv c_r(n_1, n_2), \quad r \equiv p_2 - p_1 \ . \tag{4.4}$$

Clearly, r is simply an integer in the 1D array of plaquettes, but a lattice vector of the square lattice for the 2D case.

The first approximation we make is a lowest-order local approximation in which one retains those coefficients with $|r| = 1$ only. The coefficients involved are therefore the one-plaquette coefficients $\{a_n\}$, as defined previously by Eq. (3.5), and the two-plaquette coefficients $\{b_1(n_1, n_2)\}$ and $\{c_1(n_1, n_2)\}$. One can see that there is still the mode coupling to deal with as in the SUB1 scheme. We can also make further truncations.

Within the local one-mode approximation, for example, we retain only the single coefficient, a_1, which is the same as the SUB1(1) approximation considered earlier. In the local two-mode approximation, however, four coefficients are retained. They are a_1 and a_2 from the one-plaquette equations, and $b_1(1,1)$ and $c_1(1,1)$ from the two-plaquette correlations. The equations in this particular local two-mode approximation, denoted as SUB2-1(2), are given together with the energy equation by

$$\frac{E_g}{N_p} = \lambda - a_1^2 - a_2^2 - \frac{z}{4} b_1 c_1 - \frac{z}{2}(b_1^2 + c_1^2) \ , \tag{4.5a}$$

$$-\frac{\lambda}{2} + a_1 - a_1 a_2 - z a_1 \left[b_1 + \frac{1}{4} c_1 \right] = 0 \ , \tag{4.5b}$$

$$2a_2 + \tfrac{1}{2} a_1^2 = 0 \ , \tag{4.5c}$$

$$\tfrac{1}{4}(1 - a_2) c_1 + (1 - a_2) b_1 = 0 \ , \tag{4.5d}$$

$$\tfrac{1}{4} a_1^2 + \tfrac{1}{4}(1 + a_2) b_1 + (1 + a_2) c_1 = 0 \ , \tag{4.5e}$$

where we have simplified the notation further by writing $b_1 \equiv b_1(1,1)$ and $c_1 \equiv c_1(1,1)$, and where z is the number of nearest neighbors of the lattice, i.e., $z = 2$ and 4 for the cases of 1D and 2D, respectively.

The SUB2-1(2) approximation reproduces the correct coefficients in the strong-coupling limit of the $U(1)$ models up to the fourth order [34,36]:

$$\frac{E_g}{N_p} \underset{\lambda \rightarrow 0}{\sim} \begin{cases} \lambda - \frac{1}{4}\lambda^2 + \frac{89}{3840}\lambda^4 + O(\lambda^6), & \text{1D}, \\ \lambda - \frac{1}{4}\lambda^2 + \frac{73}{3840}\lambda^4 + O(\lambda^6), & \text{2D} \ . \end{cases} \tag{4.6}$$

In a similar fashion the local three-mode approximation, the SUB2-1(3) scheme, and other local higher-order multimode approximations, can also be made within the SUB2 equations. The SUB2-1(3) scheme in particular retains seven independent coefficients. The three additional coefficients are a_3, $b_1(1,2)[= b_1(2,1)]$, and $c_1(1,2)[= c_1(2,1)]$. Tables II(a) and II(b) show the results for the GS energy per plaquette for the 1D and 2D models, respectively, at various values of λ within several SUB2-1(n) schemes ($n = 2,3,4$), together with the full SUB1 results [produced by the SUB1(10) scheme to the same accuracy shown] and the results from perturbation theory of both weak- and strong-coupling limits for comparison. The agreement with other calculations [26,35] is good.

Just as the strong-coupling perturbation series of Eq. (3.14) for the GS energy of the Mathieu problem has a finite radius of convergence, it seems likely that its counterparts for the 1D and 2D cases of U(1) lattice gauge theory from Eq. (4.6) also do. Much work in modern field theory goes into attempts to analytically continue such series outside their natural boundaries. A typical recent such attempt for the (2+1)-dimensional U(1) model [39] starts from the strong-coupling perturbation series of Eq. (4.6), utilizing the known coefficients out to $O(\lambda^{18})$, as input to generalized Padé approximants. These results are also included in Table II(b) for comparison. As stated in the previous section for the one-

TABLE II. (a) Ground-state energy per plaquette at various values of λ for the U(1) model in 1+1 dimensions. Shown are the results of the SUB2-1(n) schemes with $n=2$, 3, 4, defined in the text, together with the full SUB1 results [given by the SUB1(10) scheme to the accuracy shown] and the results of both strong ($\lambda\to 0$) and weak ($\lambda\to\infty$) coupling limits in perturbation theory, PT4(S) and PT(W), given by Eqs. (4.6) and (4.7). (b) Same as (a) but for the (2+1)-dimensional model and with additional results of eighth-order strong-coupling perturbation theory, PT8(S), from Ref. [34]. The results from an analytic continuation of the strong-coupling perturbation series by Hamer, Oitmaa, and Zheng [39] (HOZ) are also included.

λ	0.5	1	2	3	4	5	6
				(a)			
SUB1	0.4391	0.7724	1.2430	1.5828	1.8597	2.1000	2.3156
SUB2-1(2)	0.4389	0.7689	1.1980	1.3684	1.1115	−0.3116	−6.3126
SUB2-1(3)	0.4389	0.7703	1.2319	1.5567	1.8022	1.9833	2.1047
SUB2-1(4)	0.4389	0.7702	1.2320	1.5615	1.8243	2.0409	2.2184
PT4(S)	0.4389	0.7732	1.3708	2.6273	5.9333	13.236	27.038
PT(W)	0.5744	0.8624	1.2697	1.5822	1.8457	2.0778	2.2877
				(b)			
SUB1	0.4391	0.7724	1.2430	1.5828	1.8597	2.1000	2.3156
SUB2-1(2)	0.4386	0.7652	1.1468	1.1280	0.3019	−2.8326	−15.108
SUB2-1(3)	0.4387	0.7681	1.2216	1.5371	1.7691	1.9282	2.0153
SUB2-1(4)	0.4387	0.7681	1.2214	1.5428	1.7994	2.0123	2.1921
PT4(S)	0.4387	0.7690	1.3042	2.2898	4.8667	10.632	21.638
PT8(S)	0.4387	0.7673	1.1358	−0.7375	−20.873	−130.4	−555.7
HOZ			1.215		1.785		2.2
PT(W)	0.5627	0.8434	1.2402	1.5447	1.8015	2.0276	2.2321

plaquette approximation (i.e., Mathieu problem), we again emphasize that our own SUB2-1(n) approximants themselves represent a natural extension of perturbation theory. They comprise, in effect, a well-defined analytic continuation or resummation of perturbation theory results within the context of a natural and consistent hierarchy of approximations. They may be contrasted with the rather *ad hoc* approaches based on Padé and other resummation techniques, which usually find it difficult to approach the weak-coupling limit with the correct asymptotic form unless this is built in from the start.

Finally, the perturbation theory in the weak-coupling limit gives

$$\frac{E_g}{N_p}\underset{\lambda\to\infty}{\sim} C_0\sqrt{\lambda}-\frac{1}{8}C_0^2+O(\lambda^{-1/2})\ , \tag{4.7}$$

where the values of the constant C_0 are 0.9833 in 1D [36], and 0.9581 in 2D [26]. We note that the zero-dimensional analogue (namely, the Mathieu problem) has a similar weak-coupling limit, but with $C_0=1$. As can be seen from Table II, the SUB2-1(2) results are not much better than their counterparts from perturbation theory, as is the case for the SUB1(1) scheme for the Mathieu equation. However, the SUB2-1(3) and SUB2-1(4) results are very much improved. It demonstrates again that to produce correct numerical results in the weak-coupling (large λ) region, the higher-order mode-couplings are necessary.

Different sub-approximation schemes can also be made from the SUB2 equations. For example, one can include only low-mode coupling but retain long-range plaquette-plaquette correlation. Thus, one might retain the coefficients $b_r(1,1)$ and $c_r(1,1)$ with all possible values of r. From the experience of the application of the CCM to spin lattice models [25] this approximation can predict a possible phase transition. Our preliminary results do not suggest a critical behavior for any finite value of λ. This seems to agree with the general consensus that no phase transition exists for the U(1) lattice gauge model in either 1D or 2D.

V. U(1) PLAQUETTE ENERGY

In order to calculate the GS expectation value of any physical operator in the CCM, one needs to calculate the GS ket and bra wave functions separately. The CCM parametrization of the ground bra state for the U(1) model is given by Eq. (2.6), where as can be seen, $\langle\tilde{\Psi}_0|$ is not manifestly the Hermitian conjugate of $|\Psi_0\rangle$. The equations for the one-plaquette bra-state coefficients $\tilde{\mathcal{S}}_p(n)$, for example, are derived from the second variational equation of Eq. (2.9).

In this section we focus on the SUB1 scheme only, i.e., $\tilde{S}\to\tilde{S}_{\rm SUB1}=\tilde{S}_1$. From Eq. (2.9), one can derive the following equation for the one-plaquette bra-state coefficients $\{\tilde{S}_p(n)\}$ as

$$\langle\Phi|\tilde{S}_{\rm SUB1}e^{-S_{\rm SUB1}}[H,\cos mB_p]e^{S_{\rm SUB1}}|\Phi\rangle=0\ ,\qquad m=1,2,\ldots, \tag{5.1}$$

which may be compared with its ket-state counterpart of Eq. (3.1). Explicit evaluation of Eq. (5.1) readily yields

$$-2a_m+m\tilde{a}_m-\sum_{n=-\infty}^{\infty}a_n\tilde{a}_{m-n}=0\ ,\quad m=\pm1,\pm2,\ldots,\tag{5.2}$$

where a_m is defined as before by Eq. (3.5) and $\tilde{a}_m$ is defined as

$$\tilde{a}_m\equiv\tilde{\mathcal{S}}_p(m),\quad \tilde{a}_{-m}=\tilde{a}_m\ ,\tag{5.3}$$

again independent of the index p. As for the analogous ket-state equation (3.6), Eq. (5.2) is also valid for any dimension in this one-plaquette approximation.

A similar SUB1(n) subtruncation approximation to that discussed in Sec. III may also be employed for the bra-state coefficients. Thus, in this SUB1(n) scheme, one retains those coefficients $\{a_m,\tilde{a}_m\}$ with $m\le n$, and sets all others to zero. For example, in the SUB1(1) scheme, we have

$$\text{SUB1(1)}:\ \tilde{a}_1=2a_1=\lambda\ .\tag{5.4}$$

As for the earlier case of the coefficients $\{a_m\}$, it is not difficult to obtain numerical solutions to Eq. (5.2) for $\{\tilde{a}_m\}$, taking $\{a_m\}$ as known parameters, in a general SUB1(n) scheme with any finite n.

After determination of both the ket- and bra-state coefficients, we can calculate any physical quantity within the corresponding approximation. Here, as an example, we calculate the plaquette energy, which is defined by

$$U\equiv\langle 1-\cos B_p\rangle=\langle\tilde{\Psi}_0|(1-\cos B_p)|\Psi_0\rangle\ ,\tag{5.5}$$

where U is independent of the plaquette index p because of the translational invariance of the system. Within the SUB1 scheme under discussion, U is given by

$$\text{SUB1}:\ U=1-\tfrac{1}{2}\tilde{a}_1\ ,\tag{5.6}$$

and hence depends only on the single coefficient $\tilde{a}_1$. As for the GS energy, the value of U as a function of λ can be obtained numerically within the SUB1(n) scheme for any finite n. This, in effect, reproduces the corresponding exact results for the Mathieu problem. Hence, we will not quote them here, except to mention, for example, that in the strong-coupling limit, the SUB1(3) scheme gives

$$U\underset{\lambda\to0}{\sim}1-\tfrac{1}{2}\lambda+\tfrac{7}{64}\lambda^3-\tfrac{29}{768}\lambda^5+O(\lambda^7)\ ,\tag{5.7}$$

which agrees exactly with the first derivative of the GS energy, E_g/N_p, of Eq. (3.14), with respect to λ, as expected. More generally, the SUB1(n) evaluation of U from Eqs. (5.2) and (5.6) again agrees with the corresponding result from $2n$th-order perturbation theory, PT($2n$).

We note that these findings illustrate the more general result that the CCM always gives agreement with the exact Hellmann-Feynman theorem at *all* levels of truncation with consistent approximations for both correlation operators S and $\tilde{S}$. Indeed, this preservation of consistency with the Hellmann-Feynman theorem is the prime motivation for the particular parametrization of the ground bra state given by Eq. (2.14) [7]. By contrast, an approximation scheme which preserves Hermiticity between the ket and bra states at all levels of approximation would be inconsistent with this important theorem, except in the exact limit when no truncation was made for the correlation operator S.

VI. $Z(2)$ LATTICE GAUGE MODEL

In Sec. II we have given the exact CCM forms for the ket and bra states of the $Z(2)$ model by Eqs. (2.12)–(2.14). Although we could now perform a SUBn sequence of approximations for the $Z(2)$ model as outlined above for the $U(1)$ model, we prefer here, partly for pedagogical reasons, to employ a different hierarchy of approximation schemes, which we call the LSUBn sequence. This scheme, which has no simple counterpart for continuous extended systems, has been recently developed within the context of quantum spin-lattice models [25], where it has met with considerable success. It is particularly suited for treating lattice systems where the interaction forces are highly localized (i.e., short ranged).

In this spirit, we may rewrite the correlation operators $S,\tilde{S}$ for the $Z(2)$ model in the form

$$\begin{aligned}S&=\sum_p\sum_c\mathcal{S}_cU_p(c)\ ,\\ \tilde{S}&=1+\sum_p\sum_c\tilde{\mathcal{S}}_cU_p(c)\ ,\end{aligned}\tag{6.1}$$

where $U_p(c)$ is a product of σ_3 operators around a particular lattice contour of shape and orientation specified by the index c, and where the index p labels some one particular plaquette in a specified ordering of the plaquettes inside c. We note that the c-number cluster amplitudes $\{\mathcal{S}_c,\tilde{\mathcal{S}}_c\}$ are independent of either the index p or the orientation of the contour c due to invariance properties of the lattice. We also note that in rewriting Eqs. (2.12)–(2.14) in the form of Eq. (6.1), we have used that since $\sigma_3^2=1$, the product of operators U_p for any set of contiguous elementary plaquettes is equivalent to a product of $\sigma_3(l)$ operators around the links forming their boundary contour.

In the (2+1)-dimensional model, a given LSUBn approximation includes in the set $\{c\}$ all possible closed (not necessarily connected) contours which lie inside the closed, connected contours formed by all distinct groups of n contiguous elementary plaquettes on the lattice. Figure 5 shows the lowest three approximations in this scheme in diagrammatic form.

In order to evaluate the GS energy expectation value $\bar{H}$ of Eq. (2.8), one needs to calculate the similarity transform $e^{-S}He^{S}$. As usual, we utilize the well-known nested commutator expansion

$$e^{-S}He^{S}=H+[H,S]+\frac{1}{2!}[[H,S],S]+\cdots\ .\tag{6.2}$$

However, whereas the infinite expansion of Eq. (6.2) usually terminates, in practice, for most standard many-body problems [12,25] [and, in particular, it terminates at the second order for the U(1) model considered in previous sections], this is *not* the case here.

Nevertheless, for the $Z(2)$ model under consideration, the nonterminating expansion of Eq. (6.2) can readily be

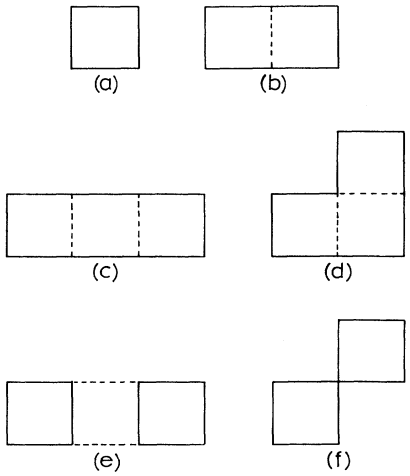

FIG. 5. The six configurations retained in the LSUB3 scheme for the $Z(2)$ model in $2+1$ dimensions. The LSUB1 scheme retains only the single configuration (a), and the LSUB2 scheme the two configurations (a) and (b).

resummed. Thus, for a general correlation operator S of the form given in Eq. (6.1), we find that

$$e^{-S}He^{S}=-\sum_{l}[\sigma_1(l)\cosh G-i\sigma_2(l)\sinh G]-\lambda\sum_{p}U_p\ , \tag{6.3}$$

where the operator G is defined by

$$G\equiv 2\sum_{p\ni l}\sum_{c}\mathcal{S}_c U_p'(c;l)\ , \tag{6.4}$$

wherein the sum over plaquettes is restricted to those which include the links l, and where $U_p'(c;l)$ is identical to the product of σ_3 operators comprising $U_p(c)$ except that the single operator $\sigma_3(l)$ on the particular link l is omitted and the ordering of the plaquettes inside c is relaxed. Both the terms $\cosh G$ and $\sinh G$ in Eq. (6.3) can then be expanded using the usual expansion rules for $\cosh(A+B)$ and $\sinh(A+B)$. Finally, using $[U_p'(c;l)]^2=1$ for all c, p, and l, since $\sigma_3^2=1$, we have the relations

$$\begin{aligned}\cosh[\mathcal{S}_c U_p'(c;l)]&=\cosh\mathcal{S}_c\ ,\\ \sinh[\mathcal{S}_c U_p'(c;l)]&=U_p'(c;l)\sinh\mathcal{S}_c\ ,\end{aligned} \tag{6.5}$$

which enable us to rewrite Eq. (6.3) in a form in which the hyperbolic functions act only on the c-number amplitudes $\{\mathcal{S}_c\}$.

We quote only the final result for $\bar{H}$ for the 2D $Z(2)$ model in the LSUB1 approximation,

$$\bar{H}_{\mathrm{LSUB1}}=-\sum_{l=1}^{N_l}\left[\cosh^2(2\mathcal{S}_1)+\frac{1}{2}\tilde{\mathcal{S}}_1[\lambda-2\sinh(4\mathcal{S}_1)]\right]\ , \tag{6.6}$$

where, in writing the result as a sum over link index l only, we have used the fact that the number of links is equal to twice the number of plaquettes for the 2D square lattice, i.e., $N_l=2N_p$. As for the U(1) model, the equations for the coefficients $\mathcal{S}_1$ and $\tilde{\mathcal{S}}_1$ are derived by requiring $\bar{H}$ to be stationary with respect to them. We find

$$\text{LSUB1:}\quad \mathcal{S}_1=\frac{1}{4}\operatorname{arcsinh}\left[\frac{\lambda}{2}\right],\quad \tilde{\mathcal{S}}_1=\frac{1}{2}\frac{\lambda}{\sqrt{1+\lambda^2/4}}\ , \tag{6.7}$$

and the GS energy per link is then given as

$$\text{LSUB1:}\quad \frac{E_g}{N_l}=-\frac{1}{2}(1+\sqrt{1+\lambda^2/4})\ . \tag{6.8}$$

For the LSUB2 approximation we find in a similar fashion that

$$\begin{aligned}\bar{H}_{\mathrm{LSUB2}}=-\sum_{l}\Big[&\cosh^2(2\mathcal{S}_1)\cosh^6(2\mathcal{S}_2)+\frac{\tilde{\mathcal{S}}_1}{2}\{\lambda+\sinh(2\mathcal{S}_1)\cosh(2\mathcal{S}_1)[12\sinh(2\mathcal{S}_2)-4\cosh(2\mathcal{S}_2)]\cosh^5(2\mathcal{S}_2)\}\\&+\frac{\tilde{\mathcal{S}}_2}{2}\{\sinh^2(2\mathcal{S}_1)[2\sinh^2(2\mathcal{S}_2)+\cosh^2(2\mathcal{S}_2)]\cosh^4(2\mathcal{S}_2)-6\cosh^2(2\mathcal{S}_1)\sinh(2\mathcal{S}_2)\cosh^5(2\mathcal{S}_2)\}\Big]\ .\end{aligned} \tag{6.9}$$

As before, $\bar{H}$ is now required to be stationary with respect to each of the retained configuration coefficients. The resulting numerical solution for E_g/N_l is shown in Fig. 6, together with the corresponding LSUB1 results from Eq. (6.8).

A priori, we expect the above LSUBn approximations to be most accurate in the strong-coupling regime, where we may compare with the known perturbation theory results for the 2D $Z(2)$ model [40]:

$$\frac{E_g}{N_l}\underset{\lambda\to 0}{\sim}-1-\frac{\lambda^2}{16}-\frac{\lambda^4}{3072}-\frac{\lambda^6}{196\,608}+O(\lambda^8)\ . \tag{6.10}$$

Our LSUB1 result of Eq. (6.8) is clearly seen to agree with Eq. (6.10) to the second order. An analytic small-λ expansion for LSUB2 reproduces the result of fourth-order perturbation theory. Also, without calculating the full expression for $\bar{H}$ in the LSUB3 approximation, we have shown that the sixth-order perturbation theory result is retrieved in this approximation. Although we have not attempted a strict proof, we conjecture that the general LSUBn approximation will reproduce the results of $2n$th-order perturbation theory, PT($2n$), in this small-λ limit, for all values of n.

It is also interesting to compare the weak-coupling ($\lambda\to\infty$) limits of our LSUB1 and LSUB2 results with the corresponding results from perturbation theory in this regime [40]:

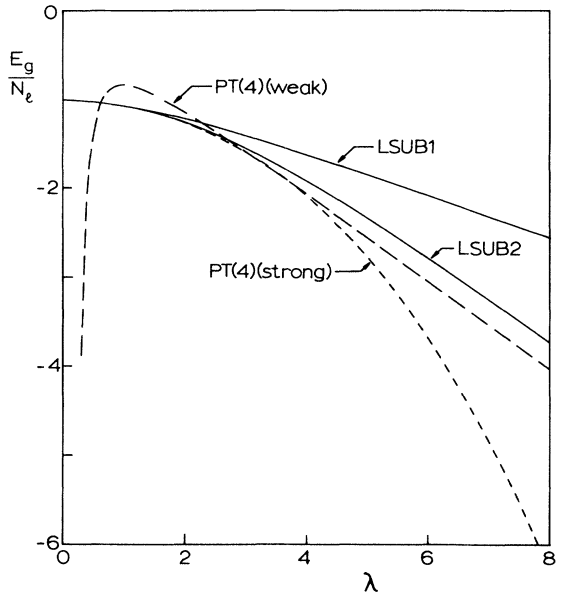

FIG. 6. Ground-state energy per link of the $Z(2)$ model in $2+1$ dimensions as a function of λ. Shown are our LSUB1 and LSUB2 results, and the fourth-order perturbation theory, PT(4), results in both the strong-coupling ($\lambda\to 0$) and weak-coupling ($\lambda\to\infty$) limits given in the text.

$$\frac{E_g}{N_l}\underset{\lambda\to\infty}{\sim}-\frac{\lambda}{2}\left[1+\frac{1}{2}\lambda^{-2}+\frac{5}{32}\lambda^{-4}+O(\lambda^{-6})\right]. \tag{6.11}$$

As expected, we do not get agreement in this limit. Nevertheless, both LSUB1 and LSUB2 approximations give the correct leading asymptotic behavior, namely, linear in λ, albeit with an incorrect coefficient. More precisely, Eq. (6.8) trivially gives $E_g/N_l\to -0.25\lambda$ as $\lambda\to\infty$ in the LSUB1 approximation, whereas the leading-order LSUB2 result is $E_g/N_l\to -k\lambda$ as $\lambda\to\infty$, where

$$k=(7+3\sqrt{7})/28\approx 0.533 .$$

This LSUB2 result is rather close to the exact value of Eq. (6.11) to the same order.

VII. EXCITATIONS OF U(1) AND Z(2) MODELS

In this section we extend the CCM to the excited states of the U(1) and $Z(2)$ models. In the conventional CCM, the excited states are constructed by acting on the ground state with the excitation correlation operator X [37,12], which is partitioned in a similar fashion to the GS correlation operator S discussed in Sec. II, replacing all GS coefficients $\{\mathcal{S}_{p_1\ldots}(n_1,\ldots)\}$ with the corresponding excitation coefficients $\{\mathcal{X}_{p_1\ldots}(n_1,\ldots)\}$. Thus, the excited state $|\Psi_e\rangle$ is *linear* in X, by contrast to the ground state $|\Psi_0\rangle$ where S is in the exponentiated form. The Schrödinger equation is then written as

$$H|\Psi_e\rangle=E_e|\Psi_e\rangle,\quad \text{with } |\Psi_e\rangle\equiv X|\Psi_0\rangle=Xe^S|\Phi\rangle . \tag{7.1}$$

This formalism, first due to Emrich [41], for the excitations is identical to a more general theory based on functional derivatives [7]. We shall use Eq. (7.1) here. However, it is important to point out that in this and other cases not all elementary excitations can be constructed by an excitation operator X identical in structure to S. This is because the symmetry of the excitations can be different from that of the ground state. For example, in antiferromagnetic spin-lattice systems, the ground state is in the sector of $s^z_{\text{total}}=0$, where s_{total} is the total spin of the system, whereas the low-lying excitations have $s^z_{\text{total}}=\pm 1$ [25]. In the U(1) lattice gauge model under discussion, one has the odd-parity excitations as well as the even-parity ones. In this case the odd-parity excitation operator X^o is similar in construction to the even-parity excitation operator X^e and the GS operator S, but with each term in X^o obeying the odd-parity symmetry.

A. Excitations of the U(1) model

As stated above, there are two branches of excitations for the U(1) model, described by the even-parity correlation operator X^e and the odd-parity correlation operator X^o, respectively. Within the SUB1 approximation X^o and X^e can be written, respectively, as

$$\begin{aligned} X^o\to X^o_{\text{SUB1}}&=\sum_{p=1}^{N_p}\sum_{n=1}^{\infty}\mathcal{X}^o_p(n)\sin nB_p ,\\ X^e\to X^e_{\text{SUB1}}&=\sum_{p=1}^{N_p}\sum_{n=1}^{\infty}\mathcal{X}^e_p(n)\cos nB_p . \end{aligned} \tag{7.2}$$

As can be seen from the above equations, the proper symmetry is observed in each case. It is not difficult to generalize to higher-order approximation schemes, such as to the SUB2 approximation. However, we focus on the SUB1 scheme in this section.

From Eq. (7.1) together with the Schrödinger GS equation, and after a straightforward manipulation, it is easy to derive the following equations for the single-plaquette excitation coefficients in general:

$$\begin{aligned} &\langle\Phi|\sin mB_q e^{-S}[H,X^o]e^S|\Phi\rangle=\epsilon^o\langle\Phi|\sin mB_q X^o|\Phi\rangle ,\\ &\epsilon^o\equiv E^o_e-E_g ,\\ &\langle\Phi|\cos mB_q e^{-S}[H,X^e]e^S|\Phi\rangle=\epsilon^e\langle\Phi|\cos mB_q X^e|\Phi\rangle ,\\ &\epsilon^e\equiv E^e_e-E_g , \end{aligned} \tag{7.3}$$

and similarly for the multiplaquette excitations. The quantities E^o_e and E^e_e are the energies of the odd and even excited states, respectively. In the SUB1 approximation under discussion, we apply the truncation of Eq. (7.2) for X^o and X^e and replace S by S_{SUB1} as given by Eqs. (3.3) and (3.6). Equations (7.3) then become

$$\begin{aligned} &\left[\frac{1}{2}\epsilon^o-m^2\right]\alpha^o_m-\sum_{n=-\infty}^{\infty}na_{m+n}\alpha^o_n=0 ,\\ &\left[\frac{1}{2}\epsilon^e-m^2\right]\alpha^e_m+\sum_{n=-\infty}^{\infty}na_{m+n}\alpha^e_n=0 , \end{aligned} \tag{7.4}$$

where the SUB1 GS coefficients $\{a_n\}$ are as defined by Eq. (3.5) and determined by Eq. (3.6), and where the $\{\alpha_n\}$ are defined accordingly as

$$\alpha_n^o \equiv \mathcal{X}_p^o(n), \quad \alpha_{-n}^o = -\alpha_n^o ,$$
$$\alpha_n^e \equiv \mathcal{X}_p^e(n), \quad \alpha_{-n}^e = \alpha_n^e . \tag{7.5}$$

These coefficients are also independent of p because of the translational invariance. Together with Eq. (3.6) we can again employ the SUB1(n) scheme in which one retains only those coefficients a_m and α_m with $|m| \leq n$. Equation (7.4) becomes an eigenvalue problem where $\{a_m\}$ are taken as known parameters from Eq. (3.6). Hence the SUB1(n) approximation corresponds to an $n \times n$ matrix diagonalization.

Consider, for example, the SUB1(2) scheme in which we retain a_n and α_n with $|n| = 1,2$ only. The eigenvalue problem from Eq. (7.4) is simply to diagonalize a 2×2 matrix. We obtain the following eigenvalues for the odd-parity excitations:

$$\text{SUB1(2)} \begin{cases} \epsilon_1^o = 5 - a_1^2 - \sqrt{9 - 14a_1^2 + a_1^4} , \\ \epsilon_2^o = 5 - a_1^2 + \sqrt{9 - 14a_1^2 + a_1^4} , \end{cases} \tag{7.6}$$

where a_1 is given by Eq. (3.13). The expressions for the even-parity excitations are similar; but generally speaking, the even-parity excitation energy is higher than its counterpart of odd parity. The glueball mass m_g of lattice gauge theory is defined as the lowest excitation energy gap. Hence we have $m_g = \epsilon_1^o$ for the U(1) model.

For a general SUB1(n) scheme, we diagonalize the corresponding $n \times n$ matrix of Eq. (7.4) by a numerical technique. The solutions for the low-lying excitations within several SUB1(n) schemes are shown in Fig. 7. As can be seen from the figure, the pattern of convergence of the solution is rather rapid as n increases, and quite similar to that for the GS energy calculations discussed in Sec. III.

Since the one-plaquette approximation (i.e., the SUB1 scheme) for the U(1) model is identical to the Mathieu problem as mentioned earlier, it is interesting to compare also our results for the excitations in this sequential SUB1(n) scheme to the corresponding exact Mathieu solutions. From Ref. [29] the first excitation gaps of the Mathieu problem in the strong-coupling limit are given to the fourth order by

$$\epsilon_1^o \underset{\lambda \to 0}{\sim} 2 + \tfrac{5}{24}\lambda^2 - \tfrac{751}{27\,648}\lambda^4 + O(\lambda^6) ,$$
$$\epsilon_1^e \underset{\lambda \to 0}{\sim} 2 + \tfrac{11}{24}\lambda^2 - \tfrac{1519}{27\,648}\lambda^4 + O(\lambda^6) . \tag{7.7}$$

We have again explicitly verified that our SUB1(3) scheme reproduces these results. Furthermore, the SUB1(3) scheme also reproduces the correct results for the second and the third excitations, ϵ_2 and ϵ_3, but to a lower order, i.e., to the orders of λ^2 for ϵ_2 and of λ^0 for ϵ_3, respectively. This suggests the following general picture: Our SUB1(n) scheme reproduces the exact perturbation results in the strong-coupling ($\lambda \to 0$) limit for the excitation gaps of the corresponding Mathieu problem to the $2(n-1)$th order in λ for the first gap, ϵ_1, $2(n-2)$th order for ϵ_2, and so on until finally to the zeroth order for ϵ_n.

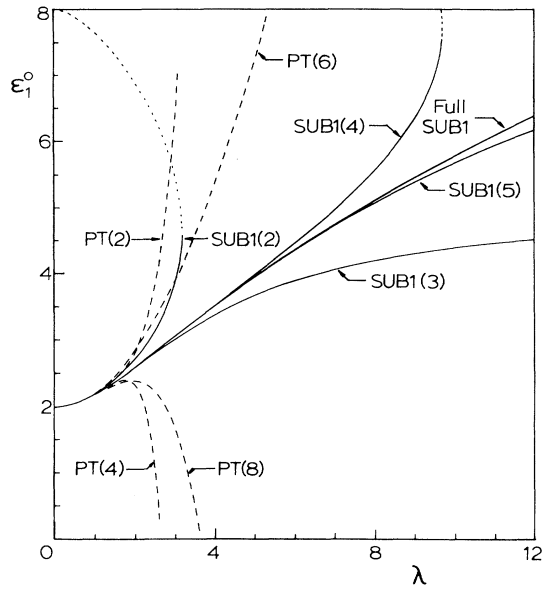

FIG. 7. The first odd-parity excitation gap, ϵ_1^o, of the U(1) model within various SUB1(n) schemes, compared with the exact Mathieu solutions (given by the full SUB1 scheme). The dotted sections of the curves for the SUB1(2) and SUB1(4) schemes represent the corresponding results for the second gap, ϵ_2^o, which connect to ϵ_1^o at some λ. Also shown are the results of strong-coupling ($\lambda \to 0$) perturbation theory, PT(n) with $n = 2$, 4, 6, 8.

We should also point out that without including multiplaquette correlations, as in the SUB1 scheme under consideration, one cannot expect to observe the exponentially decaying behavior for the glueball mass in the weak-coupling ($\lambda \to \infty$) limit. The plaquette correlations are included in the SUB2 scheme as discussed for the ground state in Sec. IV, but it is beyond our consideration for present introductory purposes. Nevertheless, in the remainder of this section, some local two-plaquette correlations are taken into account for the $Z(2)$ excitations in the so-called LSUB2 scheme, as we shall see in Sec. VII B.

B. Excitations of the $Z(2)$ model

We now focus our attention on the excited states of the $(2+1)$-dimensional $Z(2)$ model via the LSUBn approximation scheme discussed in Sec. V.

As mentioned in the beginning of this section, we define the linear excitation operator X to be of the same form as, and also to include the same set of contours as, the correlation operator S, i.e.,

$$X = \sum_p \sum_c \mathcal{X}_c U_p(c) , \tag{7.8}$$

where $\{\mathcal{X}_c\}$ are the excitation coefficients to be deter-

mined, and $U_p(c)$ is defined as before by Eq. (6.1). If a particular LSUBn approximation retains m independent configurations (i.e., m distinct shapes in the contour set $\{c\}$), then the CCM excitation equations will result in an $m \times m$ eigenvalue problem, with the m distinct eigenvalues corresponding to the excitation energies $\{\epsilon_i, i=1,2,\ldots,m\}$, similar to Eq. (7.4) for the U(1) model discussed earlier. Again, the glueball mass will be given by the lowest eigenvalue, ϵ_1.

From the strong-coupling perturbation theory, this glueball mass is given for the 2D $Z(2)$ model by [42]

$$m_g \underset{\lambda\to 0}{\sim} 8-\tfrac{3}{4}\lambda^2+\tfrac{73}{768}\lambda^4+O(\lambda^6) . \tag{7.9}$$

For the LSUB1 approximation we find our single excitation energy ϵ_1 given by

$$\text{LSUB1:}\quad \epsilon_1 \equiv m_g = 8\sqrt{1+\lambda^2/4} , \tag{7.10}$$

whereas an analytic small-λ expansion for the two excited states in our LSUB2 approximation gives

$$\text{LSUB2}\begin{cases} \epsilon_1 \equiv m_g \underset{\lambda\to 0}{\sim} 8-\tfrac{3}{4}\lambda^2+O(\lambda^4), \\ \epsilon_2 \underset{\lambda\to 0}{\sim} 12+\tfrac{9}{4}\lambda^2+O(\lambda^4) . \end{cases} \tag{7.11}$$

Thus, we observe that ϵ_1 is correct to the second order in λ, while ϵ_2 is correct to the order of λ^0. Thus, a similar pattern to that for the SUB1(n) excitation energies for the Mathieu problem emerges: The LSUBn scheme will produce the correct strong-coupling expansion to the $2(n-1)$th order for the first excitation energy gap (glueball mass), to the $2(n-2)$th order for the second gap, and so on.

VIII. SUMMARY AND CONCLUSION

In this paper we have developed a CCM analysis for the lattice gauge models, U(1) in $1+1$ and $2+1$ dimensions, and $Z(2)$ in $2+1$ dimensions. Several systematic truncation schemes have been employed. In particular, for the U(1) model, the mode couplings are studied in detail within both the SUB1 approximation and a local SUB2 scheme. The LSUBn sequence is also applied to the $Z(2)$ model. The GS energy, plaquette energy [for the U(1) model], and the excitation energies (e.g., glueball mass) are calculated as functions of the coupling constant λ for both models. Comparisons with other theories, particularly the strong-coupling perturbation series and its extensions, are made and discussed in great detail.

We note that the underlying simplicity of the $Z(2)$ model in $2+1$ dimensions renders it particularly amenable to various variational approaches using several classes of trial wave functions. In particular, it is of special interest here to note that Cardy and Hamber [43] and also Suranyi [44] have used a trial GS wave function of precisely our LSUB1 form, within the context of a standard Rayleigh-Ritz approach using an energy expectation value based on bra and ket trial states which are manifestly the Hermitian conjugates of each other. We note that such an approach reproduces the exact leading behavior of the GS energy in both the strong- and weak-coupling limits. It also very straightforwardly leads to a second-order phase transition at a critical value, $\lambda_c = 4$. Similarly, by employing a larger class of variational trial wave functions with great similarity (but not identical) to our LSUBn sequence, Dagotto and Moreo [45] were able to obtain a sequence of approximants for λ_c which, however, showed only very slow convergence to the "exact" limit as the number of retained configurations increased.

Although our own CCM results presented here for the $(2+1)$-dimensional $Z(2)$ model show no sign of a phase transition, we note that we have employed a fixed and very simple form for the uncorrelated or model state $|\Phi\rangle$. In a very general context Kümmel [46] has shown how the coupled-cluster methodology employed here can be extended to find new "maximum-overlap" single-body orbitals near a shape or phase transition. The lowest-order implementation of this scheme leads to an uncorrelated state which is essentially that of "mean-field theory." For example, for a many-fermion system, this is simply Hartree-Fock theory. For the present case it is just the variational single-plaquette LSUB1 result referred to above. It will be of considerable interest to pursue this analysis further in future work. An alternative extension of the so-called normal (NCCM) version of the CCM employed here, which also seems to be particularly well adapted in general for systems which display such phenomena as phase transitions, spontaneous symmetry breaking, and topological excitations, is the extended (ECCM) version of the theory. The application of this approach would take us too far afield for present purposes. Nevertheless, the interested reader is referred to the literature [7,10,20] for a discussion of this very powerful method.

From the preliminary results presented to date, however, it should be apparent that the key advantage of the CCM for the lattice gauge models, as for systems in quantum many-body theory to which it has already received wide applications, lies in its systematic microscopic approach. The method is manifestly nonperturbative from the outset, although, as we have shown, easy contact can be made with perturbation theory. We have demonstrated, furthermore, that even at relatively low levels of implementation the method provides accurate results far outside the realm of validity of perturbation theory. In this sense the method provides a very natural and automatic extension of the perturbative results. By contrast, Padé and similar resummation techniques can be extremely unreliable, particularly when no or only limited information is available for the asymptotic behavior in the continuum (weak-coupling) limit. From this point of view, the application of the CCM to more realistic gauge field theories is an obvious next step. For example, we intend to extend the present calculations, ourselves, both to the U(1) model in $3+1$ dimensions, as well as to such non-Abelian models as SU(2).

Finally, we note that the coupled-cluster methodology is sufficiently simple and physically well motivated as to make its extensions to even higher orders of implementation straightforward, in principle. Naturally, the actual

coupled equations for the retained cluster configuration coefficients rapidly become awkward and time consuming to generate by hand. Nevertheless, they are extremely amenable to generation by computer-algebraic techniques. Furthermore, although the resulting coupled sets of nonlinear equations appear *a priori* to be mathematically complicated (e.g., the possibility of multiple solutions exists), all of our practical experience from applications both to lattice gauge theory and to diverse systems of condensed matter, indicates that the CCM equations are extremely robust and simple to solve in practice. For example, a (unique) physical ground-state solution is almost always found in a very few iterations, by even the simplest numerical algorithms. A corollary is that any instability (e.g., the disappearance of the solution at some critical value of a coupling constant, such as that found in our earlier calculations [25] of the anisotropic Heisenberg spin-lattice model) that does arise is likely to be of physical origin rather than a mathematical artifice. For all of these reasons we believe that the CCM merits further consideration for use on problems in lattice gauge theory.

ACKNOWLEDGMENTS

One of us (R.F.B.) gratefully acknowledges support for this work in the form of a research grant from the Science and Engineering Research Council (SERC) of Great Britain. We also wish to express our gratitude to R. Guardiola and J. Navarro for useful discussions.

[1] J. W. Clark and E. Feenberg, Phys. Rev. **113**, 388 (1959); H. W. Jackson and E. Feenberg, Ann. Phys. (N.Y.) **15**, 266 (1961).

[2] F. Coester, Nucl. Phys. **7**, 421 (1958); F. Coester and H. Kümmel, *ibid.* **17**, 477 (1960).

[3] J. Čižek, J. Chem. Phys. **45**, 4256 (1966); Adv. Chem. Phys. **14**, 35 (1969).

[4] J. Paldus, J. Čižek, and I. Shavitt, Phys. Rev. A **5**, 50 (1972).

[5] R. F. Bishop and K. H. Lührmann, Phys. Rev. B **17**, 3757 (1978).

[6] H. Kümmel, K. H. Lührmann, and J. G. Zabolitzky, Phys. Rep. **36C**, 1 (1978).

[7] J. Arponen, Ann. Phys. (N.Y.) **151**, 311 (1983).

[8] H. G. Kümmel, in *Nucleon-Nucleon Interaction and Nuclear Many-Body Problems,* edited by S. S. Wu and T. T. S. Kuo (World Scientific, Singapore, 1984), p. 46.

[9] R. F. Bishop and H. G. Kümmel, Phys. Today **40** (3), 52 (1987).

[10] J. Arponen, R. F. Bishop, and E. Pajanne, Phys. Rev. A **36**, 2519 (1987); **36**, 2539 (1987); in *Condensed Matter Theories,* edited by P. Vashishta, R. K. Kalia, and R. F. Bishop (Plenum, New York, 1987), Vol. 2, p. 357.

[11] R. J. Bartlett, J. Phys. Chem. **93**, 1697 (1989).

[12] R. F. Bishop, Theor. Chim. Acta **80**, 95 (1991).

[13] K. G. Wilson, in *Lattice '89,* Proceedings of the International Symposium, Capri, Italy, 1989, edited by R. Petronzio *et al.* [Nucl. Phys. B (Proc. Suppl.) **17**, 82 (1990)].

[14] R. J. Bartlett, Theor. Chim. Acta **80**, 71 (1991). Note also that issues 2–6 of this volume are wholly devoted to articles on the CCM in the context of electronic correlations in many-electron systems.

[15] B. Day, Phys. Rev. Lett. **47**, 226 (1981); B. Day and J. G. Zabolitzky, Nucl. Phys. **A366**, 221 (1981).

[16] R. F. Bishop and K. H. Lührmann, Phys. Rev. B **26**, 5523 (1982); K. Emrich and J. G. Zabolitzky, *ibid.* **30**, 2049 (1984).

[17] K. H. Lührmann, Ann. Phys. (N.Y.) **103**, 253 (1977); H. G. Kümmel, Nucl. Phys. **A317**, 199 (1979); J. Arponen, J. Phys. G **8**, L129 (1982); J. Arponen and J. Rantakivi, Nucl. Phys. **A407**, 141 (1983); N. I. Robinson, R. F. Bishop, and J. Arponen, Phys. Rev. A **40**, 4256 (1989).

[18] E. Aalto, J. S. Arponen, and R. F. Bishop, in *Condensed Matter Theories,* edited by V. C. Aguilera-Navarro (Plenum, New York, 1990), Vol. 5, p. 297.

[19] C. S. Hsue and J. L. Chern, Phys. Rev. D **29**, 643 (1984); U. B. Kaulfuss and M. Altenbokum, *ibid.* **33**, 3658 (1986); R. F. Bishop and M. F. Flynn, Phys. Rev. A **38**, 2211 (1988); R. F. Bishop, M. C. Boscá, and M. F. Flynn, Phys. Lett. A **132**, 440 (1988); Phys. Rev. A **40**, 3484 (1989).

[20] J. S. Arponen and R. F. Bishop, Phys. Rev. Lett. **64**, 111 (1990); Ann. Phys. (N.Y.) **207**, 171 (1991); Theor. Chim. Acta **80**, 289 (1991).

[21] U. Kaulfuss, Phys. Rev. D **32**, 1421 (1985); C. S. Hsue, H. Kümmel, and P. Ueberholz, *ibid.* **32**, 1435 (1985); M. Altenbokum and H. Kümmel, *ibid.* **32**, 2014 (1985); M. Funke, U. Kaulfuss, and H. Kümmel, *ibid.* **35**, 621 (1987).

[22] H. Kümmel, Phys. Rev. C **27**, 765 (1983); G. Hasberg and H. Kümmel, *ibid.* **33**, 1367 (1986).

[23] M. Roger and J. H. Hetherington, Phys. Rev. B **41**, 200 (1990).

[24] M. Roger and J. H. Hetherington, Europhys. Lett. **11**, 255 (1990).

[25] R. F. Bishop, J. B. Parkinson, and Y. Xian, Phys. Rev. B **43**, 13 782 (1991); **44**, 9425 (1991); **46**, 880 (1992); Theor. Chim. Acta **80**, 181 (1991); J. Phys.: Condens. Matter **4**, 5783 (1992).

[26] A. Dabringhaus, M. L. Ristig, and J. W. Clark, Phys. Rev. D **43**, 1978 (1991).

[27] S. A. Chin, J. W. Negele, and S. E. Koonin, Ann. Phys. (N.Y.) **157**, 140 (1984).

[28] D. Robson and D. M. Webber, Z. Phys. C **7**, 53 (1980).

[29] G. Blanch, in *Handbook of Mathematical Functions,* edited by M. Abramowitz and I. A. Stegun (U.S. GPO, Washington, D.C., 1964), p. 721. The higher-order (λ^n, $n \geq 10$) results in Eq. (3.14) were kindly provided by R. Guardiola who has written a computer code for the general coefficients in Eq. (3.14) from both perturbation theory and our CCM SUB1 scheme, Eq. (3.6).

[30] R. Guardiola (private communication).

[31] W. Langguth, Z. Phys. C **23**, 289 (1984).

[32] E. Dagotto and A. Moreo, Phys. Rev. D **31**, 865 (1985).

[33] J. Kogut, D. K. Sinclair, and L. Susskind, Nucl. Phys. **B114**, 199 (1976); V. Alessandrini, V. Hakim, and A. Krzywicki, *ibid.* **B200**, 355 (1982); C. J. Hamer and A. C. Irving, Z. Phys. C **27**, 145 (1985); D. Horn, G. Lana, and D. Schreiber, Phys. Rev. D **36**, 3218 (1987).

[34] A. C. Irving, J. F. Owens, and C. J. Hamer, Phys. Rev. D **28**, 2059 (1983).

[35] G. Bhanot and M. Creutz, Phys. Rev. D **21**, 2892 (1980);

D. W. Heys and D. R. Stump, *ibid.* **28**, 2067 (1983); T. A. DeGrand and J. Potvin, *ibid.* **31**, 871 (1985); S. E. Koonin, E. A. Umland, and M. R. Zirnbauer, *ibid.* **33**, 1795 (1986); C. M. Yung, C. R. Allton, and C. J. Hamer, *ibid.* **39**, 3778 (1989).

[36] T. Barnes and D. Kotchan, Phys. Rev. D **35**, 1947 (1987).

[37] S. D. Drell, H. R. Quinn, B. Svetitsky, and M. Weinstein, Phys. Rev. D **19**, 619 (1979); D. Horn and M. Weinstein, *ibid.* **25**, 3331 (1982); U. Heller, *ibid.* **23**, 2357 (1981); P. Suranyi, Nucl. Phys. **B225**, 77 (1983); H. Arisue, M. Kato, and T. Fujiwara, Prog. Theor. Phys. **70**, 229 (1983); D. W. Heys and D. R. Stump, Nucl. Phys. **B258**, 13 (1987).

[38] G. Lana, Phys. Rev. D **38**, 1954 (1988).

[39] C. J. Hamer, J. Oitmaa, and Zheng Weihong, Phys. Rev. D **45**, 4652 (1992).

[40] P. Pfeuty and R. J. Elliot, J. Phys. C **4**, 2370 (1971).

[41] K. Emrich, Nucl. Phys. **A351**, 379 (1981); **A351**, 397 (1981).

[42] T. Banks and D. Sinclair, Phys. Rev. D **23**, 2962 (1981).

[43] J. Cardy and H. Hamber, Nucl. Phys. **B170**, 79 (1980).

[44] P. Suranyi, Nucl. Phys. **B210**, 519 (1982).

[45] E. Dagotto and A. Moreo, Phys. Rev. D **29**, 300 (1984).

[46] H. G. Kümmel, Nucl. Phys. **A317**, 199 (1979).